



GREEN SYNTHESIS OF ZINC OXIDE NANOPARTICLES USING CARICA PAPAYA LEAF EXTRACT FOR ANTIBACTERIAL AND ANTICANCER ACTIVITY (HELA AND MCF-7 CELLS)

A. Anantharaj, PG & Research Department of Physics, Thiru. A. Govindasamy Government Arts College, Tindivanam 604307, Tamil Nadu, India.

J. Padmavathi, Department of Physics, Mailam Engineering College, Mailam, Tindivanam, Tamil Nadu, India.

G. Udhayakumar, PG & Research Department of Physics, Thiru. A. Govindasamy Government Arts College, Tindivanam 604307, Tamil Nadu, India.

R. Nithya, Department of Physics, St.Martin's Engineering College, Secunderabad, Hyderabad, Telangana 500100

B. Gokulakumar PG & Research Department of Physics, Thiru. A. Govindasamy Government Arts College, Tindivanam 604307, Tamil Nadu, India Email ID: gokulan0575@gmail.com

Abstract

In this work Zinc oxide nanoparticles (ZnO NPs) were synthesized by carica papaya leaf extract. The biosynthesized Zinc oxide nanoparticles are generally characterized using UV-vis spectroscopy, FTIR, XRD, SEM, EDAX, TEM, DLS and Antibacterial analysis. XRD reflected the pure crystalline form and the crystallite size of nanoparticles using powdered X-ray diffractometer. In UV-vis spectroscopy, the absorbance spectra of Zinc oxide nanoparticles were recorded at 361 nm. FTIR analysis confirms the presence of organic functional groups from CPLE, impacting the surface interactions of Zinc oxide. SEM and EDAX analyses provide insights into the morphological variations and elemental composition, showcasing the successful incorporation of CPLE into Zinc oxide. DLS analysis reveals a more monodisperse system in ZnO + CPLE, suggesting a size-modifying influence of CPLE. Antibacterial activity assays demonstrate a synergistic enhancement in ZnO + CPLE, particularly against *S. aureus*, *B. subtilis*, and *E. coli*. The MTT assay reveals promising anticancer activity of ZnO + CPLE against MCF-7 breast cancer cells.

Keywords:

Green synthesis, ZnO nanoparticles, XRD, SEM, TEM, FTIR, Anti-bacterial activity, Anti-cancer activity

1. Introduction

The Carica papaya leaf extract acts as a bio template and reducing agent, facilitating the formation of ZnO nanoparticles [1]. The leaf extract contains various biomolecules like phenolics, flavonoids, and polysaccharides, which bind to zinc ions and initiate their reduction to ZnO nanoparticles. These biomolecules also control the size, shape, and surface properties of the nanoparticles [2]. The phytochemicals present in the Carica papaya leaf extract attach themselves to the surface of the ZnO nanoparticles. This functionalization alters the surface properties of the ZnO nanoparticles, potentially enhancing their stability, dispersibility, and biocompatibility. It can also introduce new functionalities like antimicrobial, antioxidant, or catalytic activity [3]. The combination of ZnO nanoparticles and Carica papaya leaf extract creates a composite material with unique properties [4]. The synergistic effect of ZnO nanoparticles and the bioactive compounds from the leaf extract can lead to enhanced performance in various applications [5]. The combined effect of ZnO nanoparticles and the antimicrobial compounds from the leaf extract can make the composite effective against various pathogens [6]. The antioxidant properties of both ZnO nanoparticles and the leaf extract can be combined to create materials with enhanced free radical scavenging activity [7]. ZnO nanoparticles are known for their photocatalytic properties, which can be used for water purification, pollutant degradation, and solar energy conversion. The functionalization with Carica papaya leaf

extract can potentially improve these properties [8]. The composite material can be used for targeted drug delivery or as biosensors due to its unique properties and biocompatibility [9]. ZnO is a versatile material with a wide range of applications. It is a semiconductor with a wide band gap, making it suitable for optoelectronic devices. ZnO is also a piezoelectric material, meaning it can generate electricity when pressure is applied. It is generally considered to be safe, but there are some concerns about potential toxicity [10]. Carica papaya leaf extract (CPLE) is a rich source of bioactive compounds, including phenolics, flavonoids, and polysaccharides. These bioactive compounds can enhance the properties of ZnO, such as its antimicrobial and antioxidant activity. ZnO + CPLE has shown promise for use in a variety of applications, including antimicrobials, antioxidants, and biomedicine [11,12,13]. Overall, ZnO + CPLE are both interesting materials with a wide range of potential applications. ZnO is a versatile material with a wide range of properties, while ZnO + CPLE has the potential to be even more versatile due to the addition of bioactive compounds from CPLE.

2. Experimental

2.1 Materials

Zinc acetate dihydrate ($\text{Zn}(\text{CH}_3\text{COO})_2 \cdot 2\text{H}_2\text{O}$) and sodium hydroxide (NaOH) were used as precursors. Carica papaya leaves and deionized water were employed as solvent materials.

2.2 Biosynthesis of ZnO Nanoparticles (NPs)

Fig.1 illustrates the eco-friendly synthesis process for ZnO nanoparticles *via* green synthesis. ZnO NPs were biosynthesized by combining 50 ml of a 0.4 M aqueous solution of zinc acetate dihydrate with 5 ml of Carica papaya leaf extract. The mixture was subjected to constant stirring for 1 hour. Subsequently, 50 ml of a 0.2 M aqueous solution of NaOH was added drop-wise, followed by continuous stirring for 2 hours until a green-white suspension was formed. During the reaction, the solution was continuously agitated for an additional 3 hours. The resulting mixture was then left undisturbed at room temperature for a full day (24 hours). Afterward, it was filtered, washed three times with deionized water, and two times with ethanol. The obtained product was dried in an air oven at 90°C for 12 hours and stored in an airtight sample tube for further analysis [1,4].

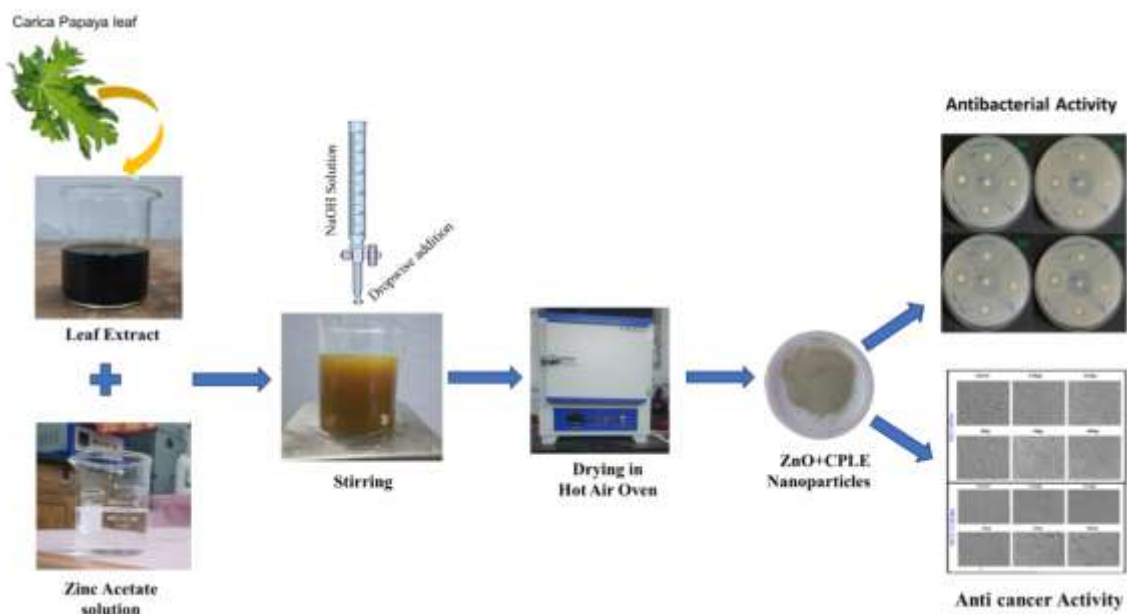


Fig.1: Depicts the process of environmentally friendly synthesis of ZnO nanoparticles through a green approach

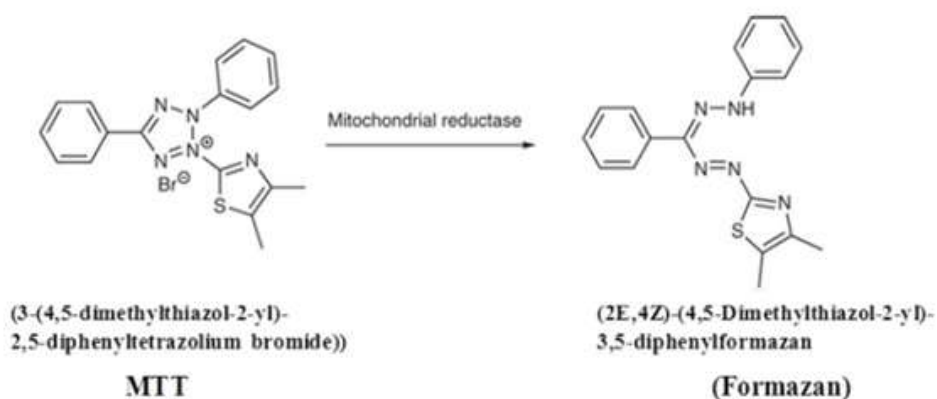
2.3 Disc-Diffusion Method

In the investigation of antibacterial activity utilizing the disc-diffusion method, the efficacy of the test samples was assessed against targeted microorganisms. To initiate the experiment, the

microorganisms were cultured in Nutrient broth and allowed to incubate for 24 hours, ensuring optimal growth conditions. Subsequently, Petri dishes containing Nutrient agar (NA) medium were utilized, and these were inoculated with a diluted bacterial strain. The test samples, prepared at concentrations of 500 µg, 1000 µg, and 2000 µg, were then applied to sterile discs, which were carefully placed onto the cultured medium. As a benchmark for comparison, the standard drug Streptomycin (20 µg) was employed as a positive reference standard to ascertain the sensitivity of the microbial species under investigation. Following the inoculation, the plates were incubated at a temperature of 37°C for a duration of 24 hours, allowing for the manifestation of antibacterial effects. The subsequent step involved measuring the diameter of the zone of inhibition that formed around each disc, providing a quantitative assessment of the antibacterial activity of the test samples. The results, expressed in millimetres, offered valuable insights into the inhibitory effects of the test substances against the target microorganisms triplicated were maintained in the experiments. This meticulously conducted disc-diffusion method thus served as a reliable means to evaluate and quantify the antibacterial potential of the test samples in this scientific study [4,5,6].

2.4 Cancer activity preparation

The MTT (3-[4, 5-dimethylthiazol-2-yl]-2, 5-diphenyl tetrazolium bromide) assay requires specific materials, including properly filtered and stored MTT reagent, DMSO, a CO₂ incubator, a microplate reader, an inverted microscope, and a refrigerated centrifuge. Test solutions were prepared by serial two-fold dilutions for the assay. HeLa cells were cultured in MEM medium containing 10% inactivated Fetal Bovine Serum, penicillin, and streptomycin, maintaining a 5% CO₂ atmosphere at 37°C until reaching confluence. The procedure involved trypsinizing the cell culture, adjusting the cell count, adding the diluted cell suspension to microtiter plates, forming a partial monolayer, and incubating with test samples. After 24 hours, MTT and DMSO were added sequentially, and absorbance was measured at 570 nm using a microplate reader [14,15,16,17,18,19,20]. Viability percentage was calculated using a specified formula.



3. Result and discussion

3.1 UV Analysis

As shown in Fig. (2), The UV-Visible spectrum of papaya leaf extract-mediated ZnO nanoparticles revealed a characteristic absorption peak at 361nm, The absorption peak observed aligned with findings from prior studies. The band gap (E_g) can be determined through a scientific formulation using the equation $E = hc/\lambda$, where E represents the energy (band gap), h is the Planck constant (6.626×10^{-34} Joules sec), c is the velocity of light (2.99×10^8 meter/sec), and λ denotes the wavelength corresponding to the absorption peak observed in UV-Vis spectroscopy. Additionally, a conversion factor of $1\text{eV} = 1.6 \times 10^{-19}$ Joules is applied [36]. The band gap energy of ZnO was determined to be 3.43 eV. Introduction of CPLE biomolecules induces subtle modifications to the UV spectrum. Interactions between CPLE components and the ZnO surface, along with potential

alterations in the electronic structure, can influence the shape and position of the band gap peak. The ZnO + CPLE composite may exhibit additional features or shoulders, contingent upon the specific energy levels of CPLE components. The band gap energy is a crucial parameter for comprehending the electronic properties of semiconductors and holds significance for their potential applications [37,38,39,40]. In the case of ZnO+CPLE composites offer a platform for tailored modifications to the band gap. The incorporation of CPLE may slightly adjust the band gap of ZnO, potentially enhancing its UV absorption spectrum. This modification could broaden the range of UV absorption, rendering the composite more efficacious for specific applications. The extent of band gap modification depends on the type and concentration of CPLE biomolecules and their interactions with the ZnO lattice [39]. Previous studies have demonstrated that incorporating organic dyes into ZnO can change its band gap, enabling the absorption of visible light. CPLE, with its diverse array of biomolecules and energy levels, provides an avenue for tailoring the UV properties of ZnO + CPLE composites. This tunability opens possibilities for designing materials with specific optical properties suited for targeted applications. In essence, understanding the Tauc plot and band gap of ZnO + CPLE provides crucial insights guiding the deliberate engineering of materials for desired optical functionalities [40,41].

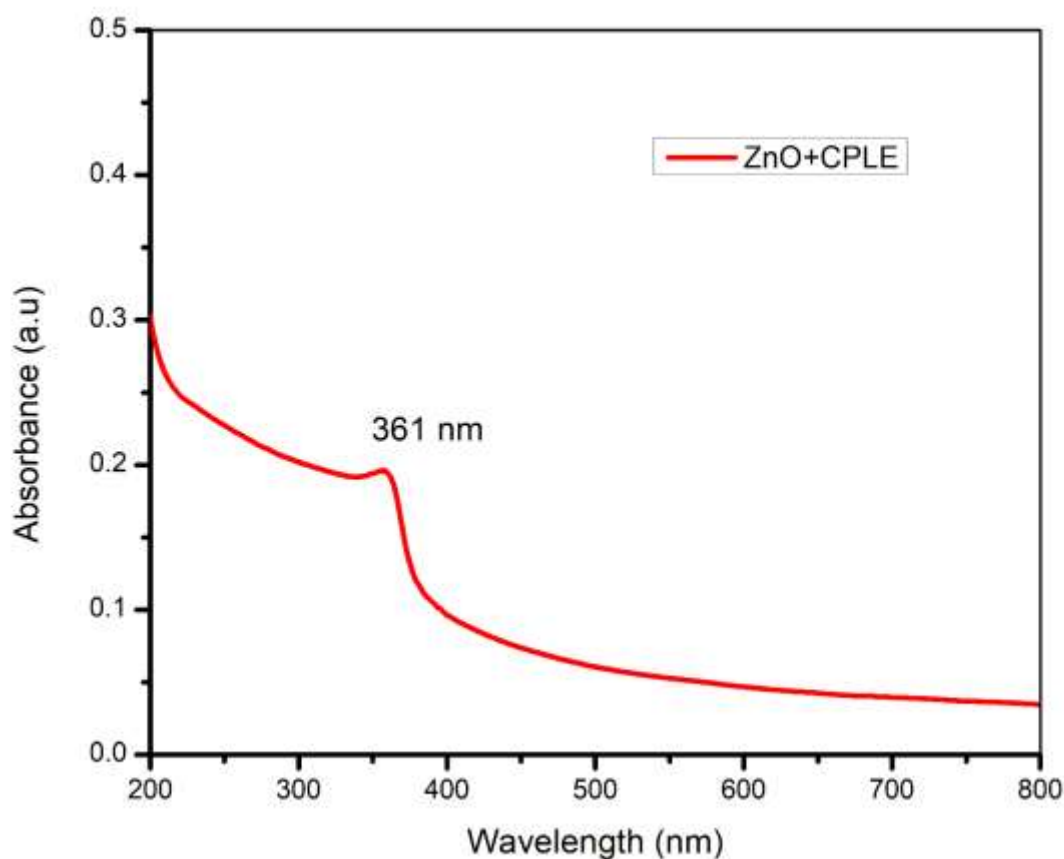


Fig. 2: illustrates the distinctive UV characteristic peaks associated with the incorporation of ZnO into CPLE

3.2 FTIR analysis

FTIR analysis serves as a crucial tool for elucidating the chemical composition and surface interactions within ZnO in conjunction with Carica Papaya Leaf Extract (CPLE), as shown in Fig.3. The FTIR spectra of ZnO + CPLE exhibit peaks at 614 cm^{-1} , 689 cm^{-1} , 1035 cm^{-1} , 1354 cm^{-1} , 1410 cm^{-1} , 1606 cm^{-1} , 2872 cm^{-1} , 2938 cm^{-1} , and 3444 cm^{-1} , reflecting the presence of organic functional groups from CPLE, such as phenols, flavonoids, and polysaccharides. The FTIR spectrum predominantly exhibits characteristic peaks, notably centred around the Zn-O stretching vibrations at UGC CARE Group-1

614 cm^{-1} - 689 cm^{-1} [31]. Peak at 3444 cm^{-1} correspond to O-H stretching vibrations of phenolic and alcoholic groups [32]. Peaks at 2872 cm^{-1} and 2938 cm^{-1} are attributed to C-H stretching of alkanes [30,32]. The band at 1606 cm^{-1} indicates C=C stretching of aromatic compounds, while peaks at 1354 cm^{-1} and 1410 cm^{-1} signify C-N stretching [33]. Moreover, peaks in the region of 1035 cm^{-1} may indicate C-O stretching [34,35]. **Table.1** shows FTIR vibration frequencies for different modes of ZnO+CPLE. in ZnO + CPLE, sharp and well-defined peaks are observed and also some peaks may exhibit broadening or attenuation, suggesting interactions between CPLE molecules and the ZnO surface. in ZnO + CPLE, the formation of new peaks is conceivable if CPLE components establish chemical bonds with ZnO. Shifts in existing peaks may result from changes in the local environment around functional groups. The presence and intensity of specific peaks provide insights into the nature of functional groups involved in bonding or adsorption. New peaks or shifts in existing peaks offer valuable information about the type and strength of interaction between ZnO and CPLE molecules. The baseline behavior can further indicate the extent of surface coverage of ZnO by CPLE components. The FTIR parameters, when interpreted collectively, furnish researchers with invaluable insights into the surface chemistry and potential functionalities of the ZnO + CPLE composite. This comprehensive analysis facilitates the identification of organic functional groups, discernment of interaction types, and quantification of surface coverage, contributing to a nuanced understanding of the material properties and potential applications of the composite.

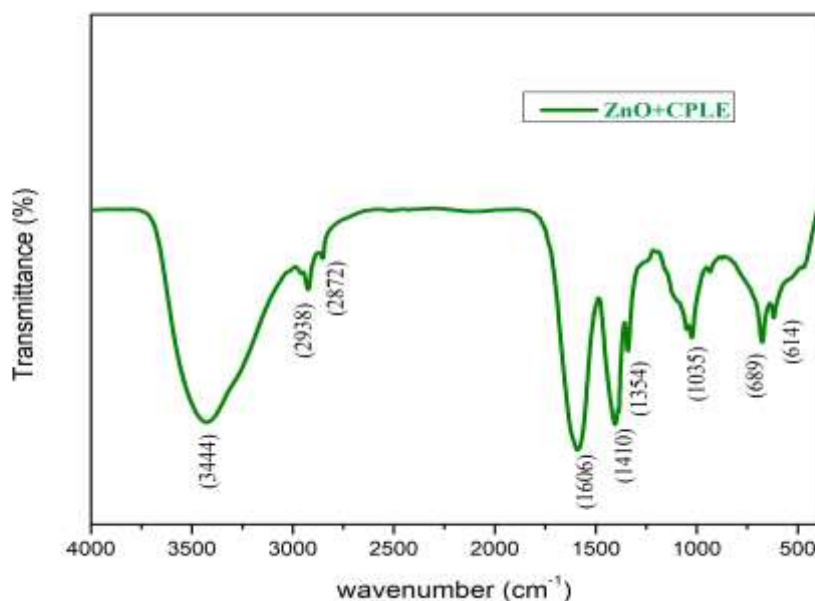


Fig. 3: illustrates the distinctive FTIR characteristic peaks observed in incorporation of ZnO into CPLE.

Table:1 FTIR Spectral peaks of synthesized ZnO NPs from fresh leaf extracts of *Carica papaya*

Absorption peak (cm^{-1}) in ZnO+CPLE NPs	Bond/functional groups	References
614, 689	Zn-O	29,31
1035	C-O Stretching	34, 35
1354, 1410	C-N Stretching (aromatic amine)	29,30
1606	C=C stretching	30
2872, 2938	C-H stretching (alkane)	30,32
3444	O-H Stretching	30,31

3.3 XRD analysis

The structural attributes of zinc oxide (ZnO) and its composite with Carica Papaya Leaf Extract (CPLE) were meticulously scrutinized through X-ray diffraction (XRD), as delineated in Fig.4. The discernible peaks associated with the ZnO+CPLE exhibited characteristic 2θ angles at 31.73° , 34.45° , 36.30° , 47.54° , 56.57° , 62.86° , 66.34° , 67.9° , and 68.9° , corresponding to the plane of (100), (002), (101), (102), (110), (004), (200), (112) and (201), aligning with the wurtzite crystal structure (JCPDS card 05-0664) [21,22,23]. A high intensity peak is observed at 101 planes, which is compared with other diffraction peaks and is designated as the characteristic peak of ZnO nanoparticles. The absence of additional diffraction peaks indicates the purity of the synthesized ZnO nanoparticles. In the ZnO + CPLE composite, indicative of lattice strain with variations for ZnO + CPLE ranging from 0.0029 to 0.0071 alterations in crystallite size/shape attributed to the interaction with CPLE [10,24,25]. Supplementary peaks in Fig.4 suggested the conceivable formation of secondary phases emanating from CPLE components. The calculated crystallite size of ZnO+CPLE, employing Scherrer's equation, spanned the range of 14-23 nm contingent upon the synthesis method. The directional predilection of ZnO for growth along specific crystal planes was juxtaposed with the contrasting influence of CPLE in ZnO + CPLE, inducing alterations in texture. XRD analysis not only yielded valuable insights into the intricate interplay between ZnO and CPLE components but also manifested discernible changes in peak positions, intensities, crystallite size, and potential secondary phases [26,27,28]. This exhaustive XRD investigation contributes indispensable information elucidating the structural and physical attributes of ZnO + CPLE. The analysis of XRD parameters facilitates the nuanced identification of crystal structure, phase purity, crystallite size, morphology, and preferred orientation, thereby enabling a comprehensive understanding of the ZnO + CPLE composite and its potential applications.

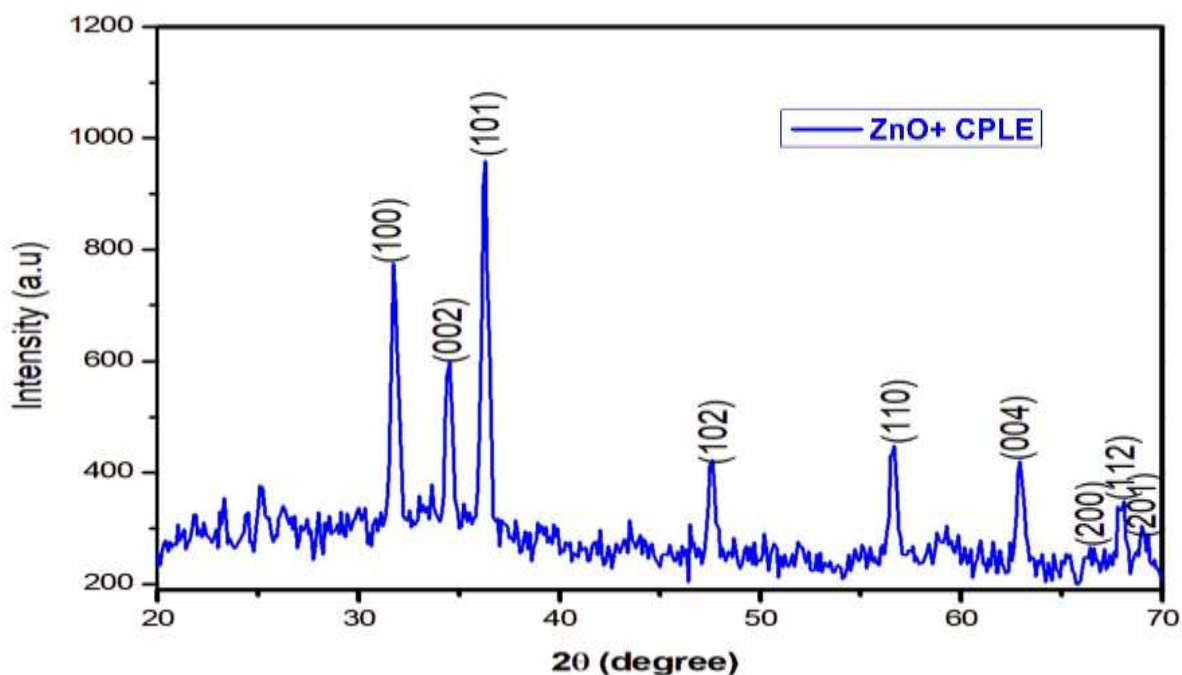


Fig.4: XRD patterns illustrating the incorporation of ZnO into CPLE.

3.4 SEM and EDAX Analysis

Scanning Electron Microscopy (SEM) is a powerful technique for investigating the morphological and elemental characteristics of materials, providing essential insights into particle size, shape, surface texture, and composition. In the context of ZnO and its composite with Carica Papaya Leaf Extract (CPLE), SEM analysis offers a detailed examination of their structural features. In Fig.5 the formation of spherical, flower shape morphology of ZnO+CPLE composites with petal like nanosheets can be observed [4,52]. ZnO + CPLE composites (Fig. 5a and b) may exhibit altered crystal growth and morphology attributed to the influence of CPLE, leading to changes in particle size and shape. Additionally, the presence of CPLE might be observable as a coating or agglomeration on the

ZnO surface. Agglomeration of ZnO nanoparticles, driven by their high surface energy, is a characteristic feature observed in ZnO. However, the introduction of CPLE in the composite can act as a stabilizer, mitigating agglomeration and improving the dispersion of ZnO nanoparticles. Energy-Dispersive X-ray Analysis (EDAX) further complements SEM observations by providing elemental composition data. In EDAX spectra ZnO + CPLE composites (Fig. 6) may show additional peaks corresponding to elements present in CPLE, such as O, C, Zn indicating the successful incorporation of organic components from CPLE into the ZnO structure. Furthermore, elemental distribution analysis through EDAX reveals insights into the uniformity of element distribution within particles. ZnO + CPLE composites may exhibit a concentration of CPLE elements on the surface of ZnO particles or a more heterogeneous distribution. This not only validates the purity of ZnO but also provides information about the incorporation and distribution of CPLE components. The combination of SEM and EDAX analyses offers a comprehensive understanding of the morphology, composition, and surface characteristics of ZnO + CPLE composites. This integrated approach enables researchers to gain valuable insights into particle size and shape variations, surface modification, and functionalization, as well as the successful incorporation of CPLE into the ZnO structure. Additionally, the EDAX analysis indicated the presence of elements such as k-shells Carbon (30.33 %), Oxygen (46.49%) and Zinc (23.18%). By interpreting these data, researchers can make informed decisions about the nature and potential applications of the ZnO + CPLE composite in various scientific and technological fields [3,4,5,42].

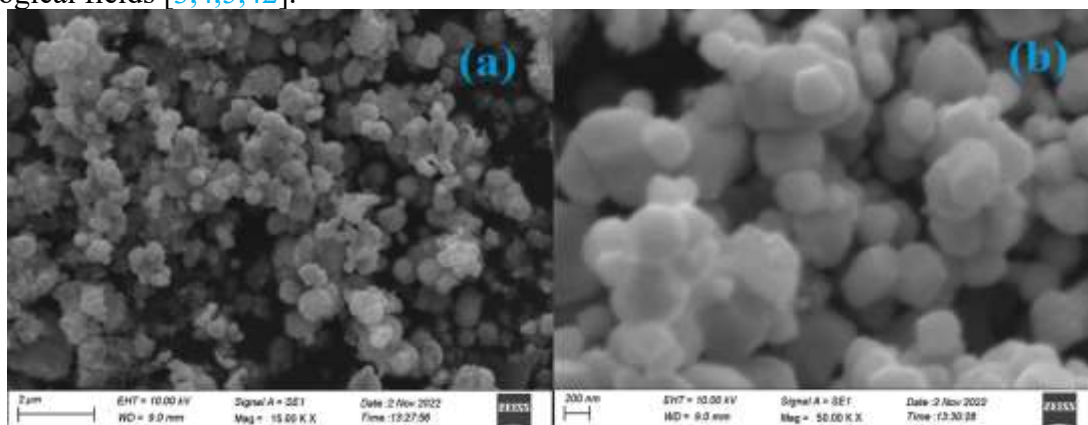


Fig. 5: Scanning Electron Microscopy (SEM) images illustrating the morphology of ZnO-incorporated CPLE (a & b)

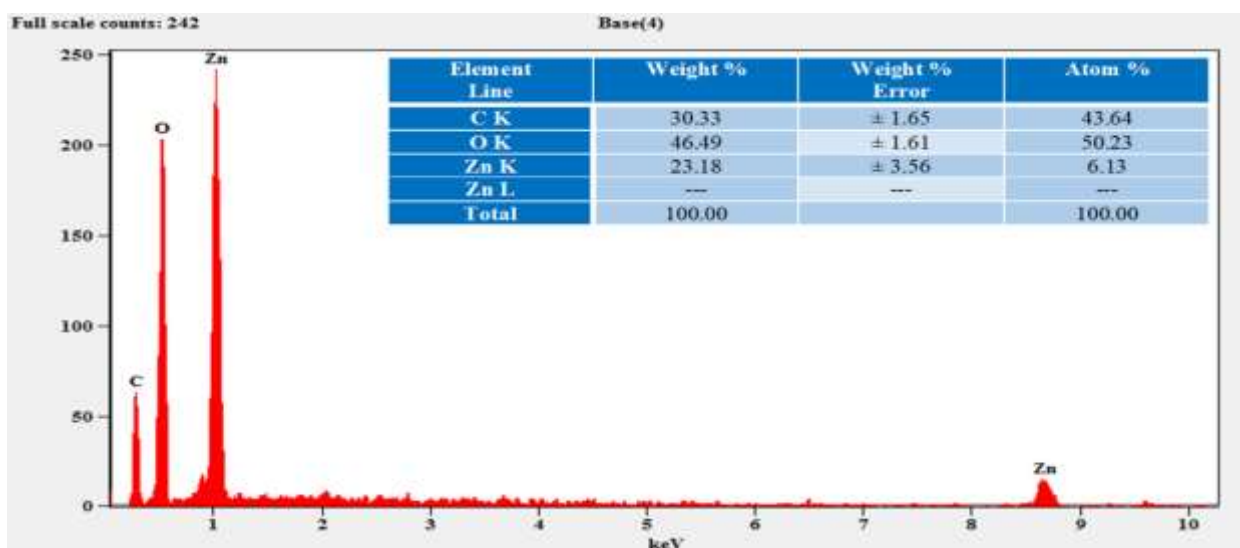


Fig.6: EDAX images illustrating the chemical element and purity of ZnO-incorporated CPLE

3.5 TEM

The Transmission Electron Microscopy (TEM) techniques were used to obtain better accuracy and determine the morphology of green synthesized ZnO nanoparticles. The average particle size of synthesized ZnO nanoparticles distributed from 14-23nm. Although most of the particles were agglomerated indicating an even distribution of the CPLE solution, a few were dispersed. From Fig.7 (a) and (b), shows agglomeration of different shaped particles such as petal-like shapes and spherical shapes [4, 52]. In TEM images of incorporation of CPLE into the ZnO NPs were covered with a thin layer of organic material from the plant extract which acted as a capping agent for stabilizing the particles [41].

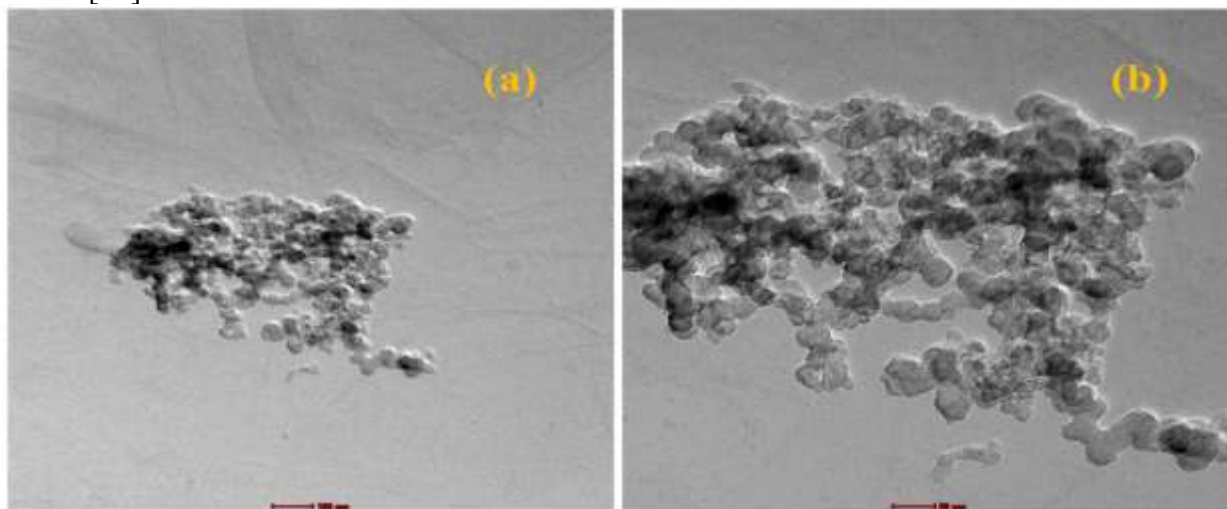


Fig. 7: a, b TEM images illustrating the morphology and size of ZnO-incorporated CPLE at 100nm and 50nm respectively

3.6 DLS Analysis

Dynamic Light Scattering (DLS) is a powerful technique used to characterize the size distribution of nanoparticles in a solution based on their Brownian motion [43]. The DLS data show an average diameter (d) of 258.7 nm with PDI of 0.371, for nanoparticles made from ZnO combined with Carica papaya leaf extract (CPLE) (Fig. 8). The DLS approach uses the hydrodynamic radius method to compute the particle size. According to the DLS the particle size is larger than that calculated using XRD due to solvation and aggregation effects in suspension.

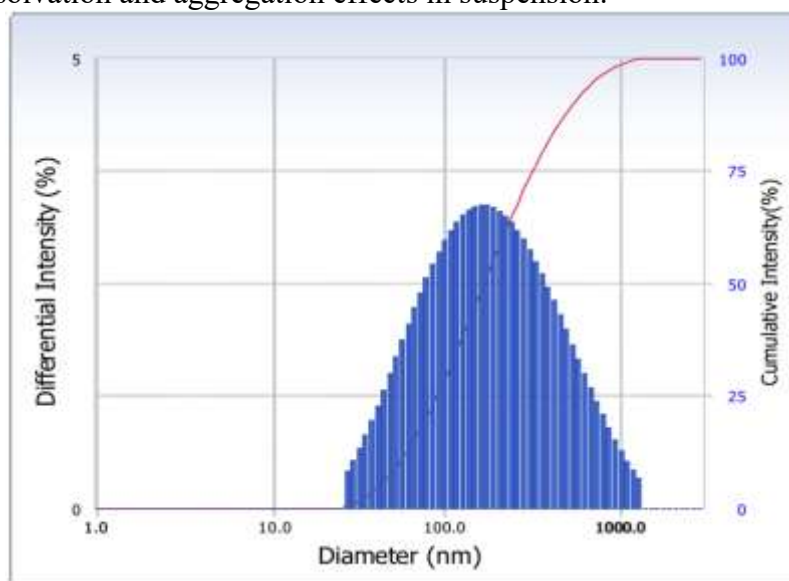


Fig.8: DLS images illustrating characterize the size distribution of nanoparticles of ZnO-incorporated CPLE

3.7 Antibacterial Activity Analysis

Certain metals exhibit strong antibacterial activity, and this property has significant implications for various applications. The antibacterial activity of metals is often attributed to their ability to release ions that are toxic to bacteria [44, 45, 46, 47, 48, 49]. ZnO + CPLE (Fig. 9) exhibit antibacterial activity against various pathogens. Table.2 presents the antibacterial activity of a combination of ZnO and Carica papaya leaf extract (CPLE) against *S. aureus*, *B. subtilis*, *E. coli*, and *P. aeruginosa* at varying concentrations (500 µg, 1000 µg, 2000 µg). Streptomycin, used as a positive control, exhibits strong antibacterial activity against all tested strains. In addition, ZnO+CPLE exhibits moderate to high antibacterial activity, with varying degrees of inhibition against different bacterial strains. The results indicate that the addition of CPLE enhances the antibacterial activity of ZnO, possibly through the presence of bioactive compounds in Carica Papaya Leaf Extract [1, 6,23,24]. Among the tested pathogens, *S. aureus* exhibited greater sensitivity to green synthesis ZnO nanoparticles, with a 14 mm zone of inhibition at the highest concentration (200 µg). Moreover *E. coli* and *P. aeruginosa* showed a moderate inhibitory zone, while *B. subtilis* showed less activity shown in Fig.10. Further studies may be needed to elucidate the specific mechanisms underlying this enhancement and explore the potential applications of the ZnO-CPLE combination in combating bacterial infections. Overall, these findings contribute valuable insights into the potential use of ZnO+CPLE as antibacterial agents and highlight the importance of combination therapies in enhancing antimicrobial efficacy.

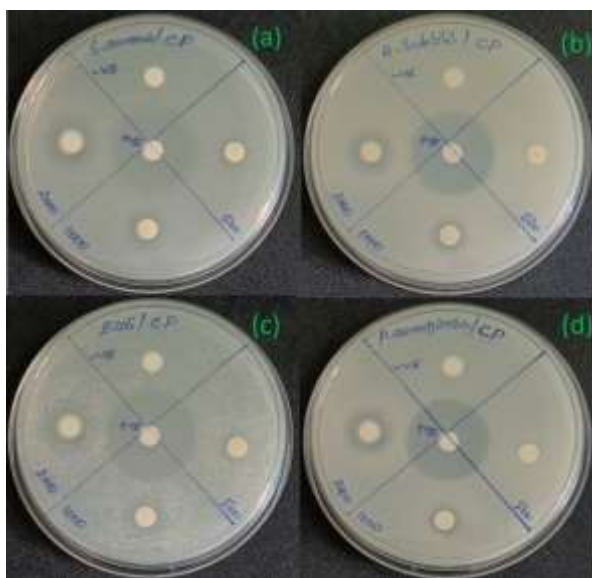


Fig.9: Antibacterial efficacy assessment of CPLE with ZnO integration against various bacterial strains, including (a) *S. aureus*, (b) *B. subtilis*, (c) *E. coli*, and (d) *P. aeruginosa*.

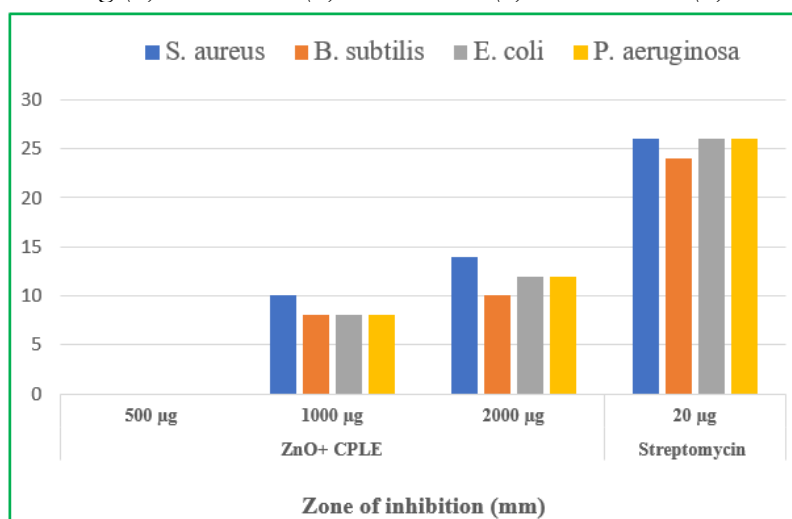


Fig.10: Zone of inhibition of CPLE with ZnO integration against various bacterial strains, including (a) *S. aureus*, (b) *B. subtilis*, (c) *E. coli*, and (d) *P. aeruginosa*. at different concentration (500 µg, 1000 µg, 2000 µg)

Table:2 ZnO + *Carica Papaya Leaf Extract (CPLE)* of antibacterial activity

Samples	Zone of Inhibition (mm)											
	Gram positive						Gram negative					
	<i>S.aureus</i>			<i>B.subtilis</i>			<i>E. coli</i>			<i>P.aeruginosa</i>		
	500 µg	1000 µg	2000 µg	500 µg	1000 µg	2000 µg	500 µg	1000 µg	2000 µg	500 µg	1000 µg	2000 µg
ZnO + <i>Carica Papaya Leaf Extract (CPLE)</i>	-	10	14	-	8	10	-	8	12	-	8	12
Streptomycin (20 µg)	26			24			26			26		

3.8 Anticancer Activity

HeLa and MCF-7 represent distinct human cancer cell lines extensively employed in biomedical investigations. HeLa originates from cervical cancer, and MCF-7 from breast cancer, each exhibiting unique characteristics and diverse responses to therapeutic interventions. The utilization of the HeLa cell line in biomedical research is widespread [15].

Evaluating cellular activity involves various methodologies, including counting viable cells stained with vital dyes or employing automated counters measuring radioisotope incorporation. The MTT assay, utilizing 3-[4, 5-dimethylthiazol-2-yl]-2, 5-diphenyl tetrazolium bromide, stands out as a precise and reproducible means to assess living cell activity via mitochondrial dehydrogenases. The assay produces a formazan by-product, whose spectrophotometric measurement reflects cytotoxicity. The impact of produced ZnO nanoparticles on HeLa cells treated with cisplatin is an understudied aspect, prompting hypotheses of enhanced sensitivity through increased DNA damage and apoptosis or reduced sensitivity via protective mechanisms like autophagy or DNA repair. Experimental validation is essential using techniques such as cell viability assays, flow cytometry, western blotting, and microscopy. For MCF-7 breast cancer cells, IC50 values for ZnO + CPLE and the reference standard (Cisplatin) were determined as >100 µg and 6.18 µg, respectively [14,15]. ZnO nanoparticles pose challenges in biomedicine, necessitating assessment of cytotoxicity and biocompatibility across diverse cell types. Studies suggest ZnO nanoparticles induce oxidative stress and apoptosis in MCF-7 cells, depending on nanoparticle characteristics. Apoptosis, a programmed cell death process, is regulated by multiple signaling pathways. Systems biology approaches, integrating gene, protein, and phosphoprotein data, aid in understanding molecular mechanisms and identifying potential therapeutic targets for breast cancer [16, 17, 18, 19].

Figs. 11 & 12 shows the microscopic images of the HeLa cell line treated with ZnO +CPLE nanoparticles and Cisplatin (reference standard) at different concentrations compared with control. Figs. 13 & 14 depicting the MCF-7 cell line treated with ZnO+CPLE nanoparticles and 5-FU (reference standard). The MTT assay serves as a valuable tool for in vitro toxicity assessments. In a study on MCF7 breast cancer cells, serial two-fold dilutions of test samples were incubated, treated with MTT, and absorbance measured, yielding IC50 values of 73.46 µg for CP and 8.18 µg for the reference standard (5FU). Fig. 15 (a, b) shows the HeLa and MCF-7 cells' survival viability at different concentrations of control (6.25, 12.5, 25, 50, and 100 µg/µL) with its reference standard. The study showcases the simplicity, accuracy, and reproducibility of the MTT method, utilizing reagents, a CO₂ incubator, a microplate reader, an inverted microscope, and a refrigerated centrifuge. This approach contributes insights into the cytotoxic activity of synthesized ZnO NPs on MCF-7 breast cancer cells [17, 18, 19, 20]. *Carica papaya leaf extract (CPLE)* is a natural product with demonstrated benefits on

platelet count and the immune system in conditions like dengue fever and chronic immune thrombocytopenic purpura. Zinc oxide (ZnO) nanoparticles, a metal oxide with potential applications in nanomedicine, exhibit properties suitable for drug delivery, imaging, and biosensing. 5-fluorouracil (5-FU), a chemotherapy drug, inhibits DNA synthesis and induces apoptosis in cancer cells. HeLa and MCF-7 cell lines, derived from cervical and breast cancers, respectively, remain pivotal in biomedical research [3, 50, 51], offering varied characteristics and responses to treatments.

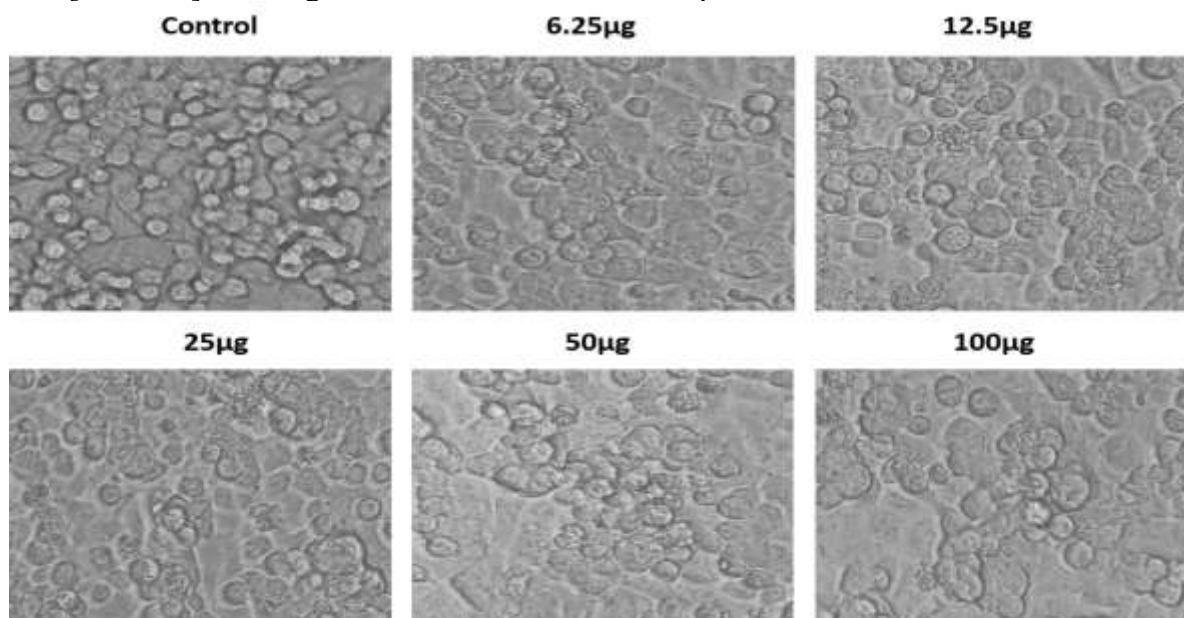


Fig. 11. Microscopic images showing the effect of ZnO+CPLE nanoparticles on HeLa cell line at different concentrations compared with control

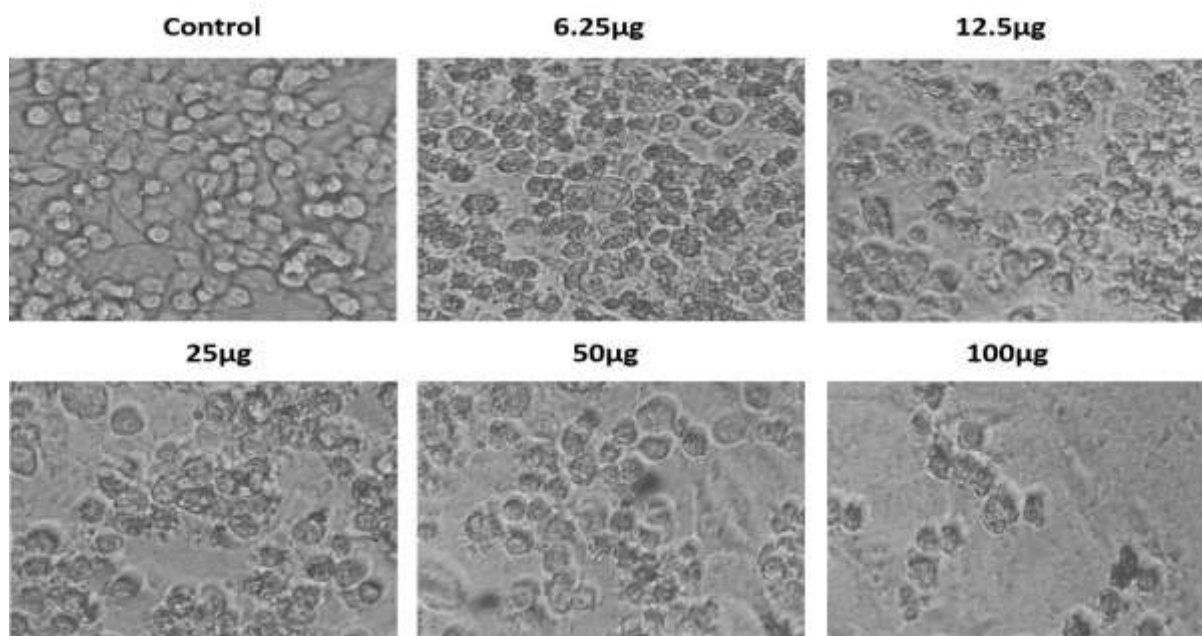


Fig. 12. Microscopic images of the HeLa cell line treated with Cisplatin (reference standard) at different concentrations compared with control

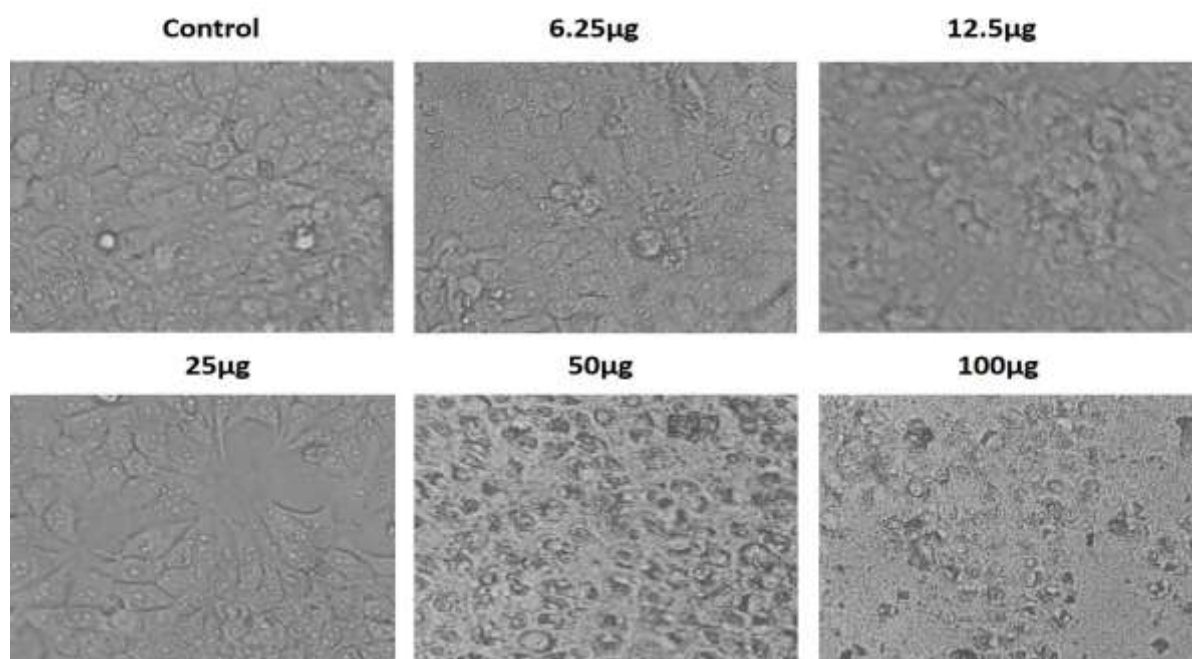


Fig. 13. Microscopic images showing the effect of ZnO+CPLE nanoparticles on MCF-7 cell line at different concentrations compared with control

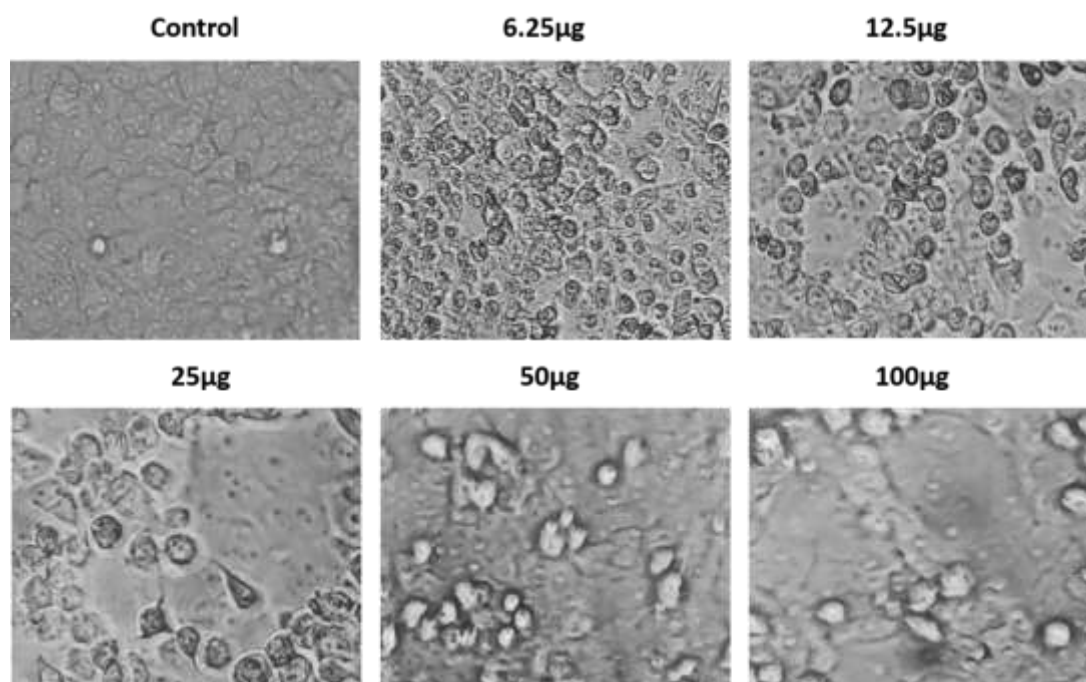


Fig. 14. Microscopic images of MCF-7 cell line treated with 5-FU (reference standard) at different concentration compared with control

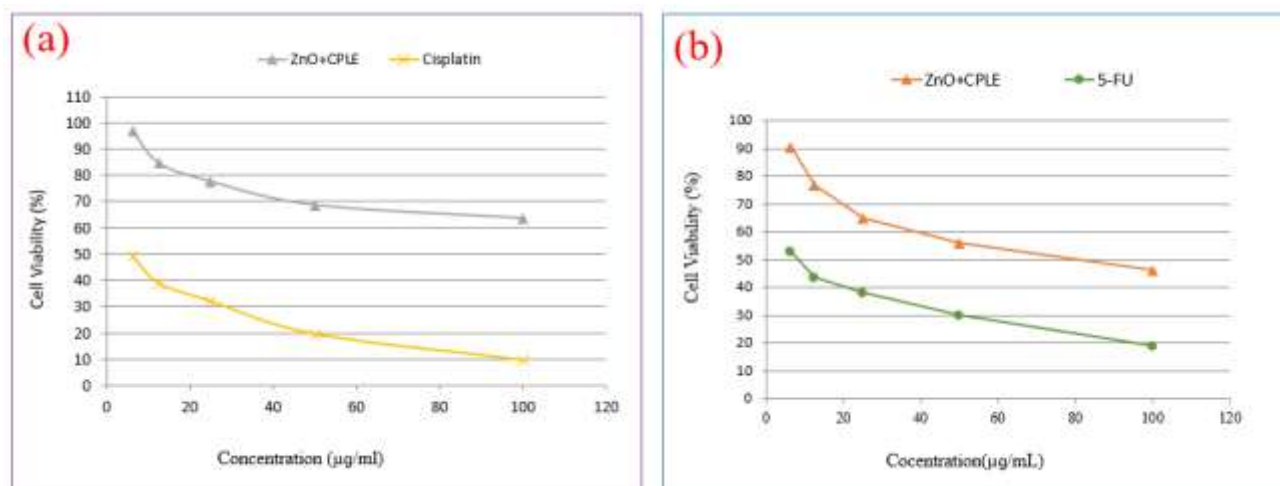


Fig.15: The decay curves of a) HeLa cell, b) MCF-7 cells survival viability at different concentration of control, 6.25, 12.5, 25, 50, 100 µg/µL with its reference standard

4. Conclusions

The present study successfully demonstrates the green synthesis of Zinc Oxide nanoparticles using carica papaya leaf extract as a reducing (ZnO+ CPLE) and stabilizing agent. The formation of ZnO NPs was confirmed by UV-Visible spectroscopy with an absorption peak around 361nm. FTIR analysis indicated the presence of phytochemicals responsible for capping and stabilization. XRD conformed the crystalline wurtzite structure of papaya leaf extract mediated ZnO NPs with an average crystallite size of ~ 15 nm, while SEM images revealed predominantly spherical, flower shape morphology with slight agglomeration and particle size in the 15-30 nm range, together validating the successful green synthesis of stable nanoscale ZnO. DLS showed PDI 0.371 for synthesised ZnO NPs have moderately uniform size distribution with good colloidal stability. The antibacterial study revealed that *S. aureus* showed the greatest antibacterial activity to the papaya leaf extract-mediated ZnO nanoparticles, followed by *E. coli*, *B. subtilis*, and *P. aeruginosa*, indicating that Gram-positive bacteria were more susceptible than Gram-negative strain. In addition, the MTT assay indicates an IC50 value of 73.46 µg for CPLE mediated ZnO NPs against MCF-7 breast cancer cells. As a result, the synergistic combination of ZnO with *Carica papaya* leaf extract presents a promising avenue for multifunctional applications with enhanced structural, optical, and biological properties.

Author's Declaration

The authors declare that they have no known competing financial interest or personal relationships that could have appeared to influence the work reported in this paper.

Data Availability Statement

All data are contained within the manuscript and supporting document

Author's Contribution Statement

- A. Anantharaj** : Conceptualization, Methodology, Data curation, Writing-original draft.
- J. Padmavathi** : Methodology, Data curation, Formal analysis, Investigation.
- G. Udhayakumar** : Methodology, Data curation, Formal analysis, Investigation.
- B. Gokulakumar** : Conceptualization, Methodology, Visualization, Validation, Supervision, Writing-review & editing.
- R. Nithya** : Methodology, Data curation, Formal analysis, Investigation.

References

- [1] Hamed, R., Obeid, R. & Abu-Huwajj, R. (2023). Plant mediated-green synthesis of zinc oxide nanoparticles: An insight into biomedical applications. *Nanotechnology Reviews*, 12(1), 20230112. <https://doi.org/10.1515/ntrev-2023-0112>



- [2] Islam, S., Bairagi, S., & Kamali, M.R. (2023). Review on Green Biomass-Synthesized Metallic Nanoparticles and Composites and Their Photocatalytic Water Purification Applications: Progress and Perspectives. *Chemical Engineering Journal Advances*. <https://doi.org/10.1016/j.ceja.2023.100460>
- [3] Rathnasamy, R., Thangasamy, P., Thangamuthu, R., Sampath, S., & Alagan, V. (2017). Green synthesis of ZnO nanoparticles using *Carica papaya* leaf extracts for photocatalytic and photovoltaic applications. *Journal of Materials Science: Materials in Electronics*, 28, 10374-10381. <https://doi.org/10.1007/s10854-017-6807-8>
- [4] Dulta, K., Koşarsoy Ağçeli, G., Chauhan, P.K., Jasrotia, R., & Chauhan, P.K. (2021). Ecofriendly Synthesis of Zinc Oxide Nanoparticles by *Carica papaya* Leaf Extract and Their Applications. *Journal of Cluster Science*, 33, 603 - 617. <https://doi.org/10.1007/s10876-020-01962-w>
- [5] Dutta, G., Chinnaiyan, S.K., Sugumaran, A., & Narayanasamy, D. (2023). Sustainable bioactivity enhancement of ZnO–Ag nanoparticles in antimicrobial, antibiofilm, lung cancer, and photocatalytic applications. *RSC Advances*, 13, 26663 - 26682. <https://doi.org/10.1039/D3RA03736C>
- [6] Gupta, M., Tomar, R.S., Kaushik, S., Mishra, R.K., & Sharma, D. (2018). Effective Antimicrobial Activity of Green ZnO Nano Particles of *Catharanthus roseus*. *Frontiers in Microbiology*, 9. <https://doi.org/10.3389/fmicb.2018.02030>
- [7] Marin-Flores, C.A., Rodríguez-Nava, O., García-Hernández, M., Ruíz-Guerrero, R., Juárez-López, F., & Morales-Ramírez, Á.D. (2021). Free-radical scavenging activity properties of ZnO sub-micron particles: size effect and kinetics. *Journal of Materials Research and Technology*. <https://doi.org/10.1016/j.jmrt.2021.05.050>
- [8] Majumder, S., Chatterjee, S., Basnet, P., Mukherjee, J., & Mukherjee, J. (2020). ZnO based nanomaterials for photocatalytic degradation of aqueous pharmaceutical waste solutions – A contemporary review. *Environmental Nanotechnology, Monitoring and Management*, 14, 100386. <https://doi.org/10.1016/j.enmm.2020.100386>
- [9] Huo, Y., Liu, Y., Xia, M., Du, H., Lin, Z., Li, B., & Liu, H. (2022). Nanocellulose-Based Composite Materials Used in Drug Delivery Systems. *Polymers*, 14. <https://doi.org/10.3390/polym14132648>
- [10] Raha, S., & Ahmaruzzaman, M. (2022). ZnO nanostructured materials and their potential applications: progress, challenges and perspectives. *Nanoscale Advances*, 4, 1868 - 1925. <https://doi.org/10.1039/D1NA00880C>
- [11] Singh, S.P., Kumar, S., Mathan, S.V., Tomar, M.S., Singh, R.K., Verma, P.K., Kumar, A., Kumar, S., Singh, R.P., & Acharya, A. (2020). Therapeutic application of *Carica papaya* leaf extract in the management of human diseases. *DARU Journal of Pharmaceutical Sciences*, 28, 735 - 744. <https://doi.org/10.1007/s40199-020-00348-7>
- [12] Khor, B., Chear, N.J., Azizi, J.B., & Khaw, K.Y. (2021). Chemical Composition, Antioxidant and Cytoprotective Potentials of *Carica papaya* Leaf Extracts: A Comparison of Supercritical Fluid and Conventional Extraction Methods. *Molecules*, 26. <https://doi.org/10.3390/molecules26051489>
- [13] Nandini, G.K., Ts, G., Prasad, N., Karthikeyan, M., Gnanasekaran, A., Ranjith, M.S., Palanisamy, P., & Basalingappa, K.M. (2020). PHYTOCHEMICAL ANALYSIS AND ANTIOXIDANT PROPERTIES OF LEAF EXTRACTS OF *CARICA PAPAYA*. *Asian Journal of Pharmaceutical and Clinical Research*. <https://doi.org/10.22159/ajpcr.2020.v13i11.38956>
- [14] Sodde, V. K., Lobo, R., Kumar, N., Maheshwari, R., & Shreedhara, C. S. (2015). Cytotoxic activity of *Macrosolen parasiticus* (L.) Danser on the growth of breast cancer cell line (MCF-7). *Pharmacognosy magazine*, 11(Suppl 1), S156. <https://doi.org/10.4103/0973-1296.157719>
- [15] Saranya, J., Sreeja, B.S., Arivanandan, M. et al. Nanoarchitectonics of Cerium Oxide/Zinc Oxide/Graphene Oxide Composites for Evaluation of Cytotoxicity and Apoptotic Behavior in HeLa and VERO Cell Lines. *J Inorg Organomet Polym* 32, 560–571 (2022). <https://doi.org/10.1007/s10904-021-02128-5>
- [16] Akhtar, M. J., Alhadlaq, H. A., Alshamsan, A., Majeed Khan, M. A., & Ahamed, M. (2015). Aluminum doping tunes band gap energy level as well as oxidative stress-mediated cytotoxicity of ZnO nanoparticles in MCF-7 cells. *Scientific reports*, 5(1), 13876. <https://doi.org/10.1038/srep13876>



- [17] Aljabali, A. A., Obeid, M. A., Bakshi, H. A., Alshaer, W., Ennab, R. M., Al-Trad, B., ... & Tambuwala, M. M. (2022). Synthesis, characterization, and assessment of anti-cancer potential of ZnO nanoparticles in an in vitro model of breast cancer. *Molecules*, 27(6), 1827. <https://doi.org/10.3390/molecules27061827>
- [18] Boroumand Moghaddam, A., Moniri, M., Azizi, S., Abdul Rahim, R., Bin Ariff, A., Navaderi, M., & Mohamad, R. (2017). Eco-friendly formulated zinc oxide nanoparticles: induction of cell cycle arrest and apoptosis in the MCF-7 cancer cell line. *Genes*, 8(10), 281. <https://doi.org/10.3390/genes8100281>
- [19] Sureshkumar, S., Jothimani, B., Sridhar, T.M. *et al.* Synthesis of Hexagonal ZnO-PQ7 Nano Disks Conjugated with Folic Acid to Image MCF – 7 Cancer Cells. *J Fluoresc* 27, 21–29 (2017). <https://doi.org/10.1007/s10895-016-1932-y>
- [20] Selvakumari, D., Deepa, R., Mahalakshmi, V., Subhashini, P., & Lakshminarayan, N. (2015). Anticancer activity of ZnO nanoparticles on MCF7 (breast cancer cell) and A549 (lung cancer cell). *ARPN J. Eng. Appl. Sci*, 10(12), 5418-5421. https://www.researchgate.net/publication/282918208_Anti_cancer_activity_of_zno_nanoparticles_on_MCF7_breast_cancer_cell_and_A549_lung_cancer_cell
- [21] Geurts, J. (2010). Crystal Structure, Chemical Binding, and Lattice Properties. In: Zinc Oxide. Springer Series in Materials Science, vol 120. Springer, Berlin, Heidelberg. https://doi.org/10.1007/978-3-642-10577-7_2
- [22] Veer, D., Singh, R.M., & Kumar, H. (2017). Structural and Optical Characterization of ZnO-TiO₂-SiO₂ Nanocomposites Synthesized by Sol-Gel Technique. *Asian Journal of Chemistry*, 29, 2391-2395. <https://doi.org/10.14233/ajchem.2017.20690>
- [23] Hu, C., Zheng, G., Zhao, F., Shao, H., Zhang, Z., Chen, N., Jiang, L., & Qu, L. (2014). A powerful approach to functional graphene hybrids for high performance energy-related applications. *Energy and Environmental Science*, 7, 3699-3708. <https://doi.org/10.1039/C4EE01876A>
- [24] Das, S., & Srivastava, V.C. (2018). An overview of the synthesis of CuO-ZnO nanocomposite for environmental and other applications. *Nanotechnology Reviews*, 7, 267 - 282. <https://doi.org/10.1515/ntrev-2017-0144>
- [25] Shinde, R.S., Khairnar, S.D., Patil, M.R. *et al.* Synthesis and Characterization of ZnO/CuO Nanocomposites as an Effective Photocatalyst and Gas Sensor for Environmental Remediation. *Journal of Inorganic and Organometallic Polymers and Materials* 1-32, 1045–1066 (2022). <https://doi.org/10.1007/s10904-021-02178-9>
- [26] Abdelouhab, Z.A., Djouadi, D., Chelouche, A. *et al.* Structural, morphological and Raman scattering studies of pure and Ce-doped ZnO nanostructures elaborated by hydrothermal route using nonorganic precursor. *J Sol-Gel Sci Technol* 95, 136–145 (2020). <https://doi.org/10.1007/s10971-020-05293-0>
- [27] Kayani, Z.N., Saleemi, F. & Batool, I. Effect of calcination temperature on the properties of ZnO nanoparticles. *Appl. Phys. A* 119, 713–720 (2015). <https://doi.org/10.1007/s00339-015-9019-1>
- [28] Rahman, A., Lalasari, L.H., Sofyan, N., Daneswara, D., & Yuwono, A.H. (2023). Investigating the effect of crystallite size on the optical properties of zinc oxide. *AIP Conference Proceedings*. <https://doi.org/10.1063/5.0116006>
- [29] Kangathara, N., Sabari, V., Saravanan, L., & Elangovan, S. (2022). Synthesis, Characterization, and Comparison of Pure Zinc Oxide and Magnesium-Doped Zinc Oxide Nanoparticles and their Application on Ethanol Sensing Activities. *Journal of Nanomaterials*. <http://dx.doi.org/10.1155/2022/1769278>
- [30] Balogun, S.W., James, O.O., Sanusi, Y.K. *et al.* Green synthesis and characterization of zinc oxide nanoparticles using bashful (*Mimosa pudica*), leaf extract: a precursor for organic electronics applications. *SN Appl. Sci.* 2, 504 (2020). <https://doi.org/10.1007/s42452-020-2127-3>



- [31] Patel, M., Mishra, S., Verma, R. et al. Synthesis of ZnO and CuO nanoparticles via Sol gel method and its characterization by using various technique. *Discov Mater* 2, 1 (2022). <https://doi.org/10.1007/s43939-022-00022-6>
- [32] Pawley, A.R., Jones, R.L. Hydroxyl stretching in phyllosilicates at high pressures and temperatures: an infrared spectroscopic study. *Phys Chem Minerals* 38, 753–765 (2011). <https://doi.org/10.1007/s00269-011-0448-x>
- [33] Faghihzadeh, F., Anaya, N.M., Schifman, L.A. et al. Fourier transform infrared spectroscopy to assess molecular-level changes in microorganisms exposed to nanoparticles. *Nanotechnol. Environ. Eng.* 1, 1 (2016). <https://doi.org/10.1007/s41204-016-0001-8>
- [34] Parlak, C., Ramasami, P. Theoretical and experimental study of infrared spectral data of 2-bromo-4-chlorobenzaldehyde. *SN Appl. Sci.* 2, 1148 (2020). <https://doi.org/10.1007/s42452-020-2935-5>
- [35] Faisal, S., Jan, H., Shah, S.A., Shah, S., Khan, A.A., Akbar, M.T., Rizwan, M., Jan, F., Wajidullah, Akhtar, N., Khattak, A., & Syed, S. (2021). Green Synthesis of Zinc Oxide (ZnO) Nanoparticles Using Aqueous Fruit Extracts of *Myristica fragrans*: Their Characterizations and Biological and Environmental Applications. *ACS Omega*, 6, 9709 - 9722. <https://doi.org/10.1021/acsomega.1c00310>
- [36] R. Paschotta, article on "Band Gap" in the RP Photonics Encyclopedia, retrieved 2024-01-04, <https://doi.org/10.61835/9f5>
- [37] Faraj, M.G., Ahmed, D.R. Photoelectrochemical study of zinc oxide (ZnO) thin films on different polymer substrates by sputtering technique. *Indian J Phys* (2023). <https://doi.org/10.1007/s12648-023-02960-0>
- [38] Viezbicke, B.D., Patel, S., Davis, B.E., & Birnie, D.P. (2015). Evaluation of the Tauc method for optical absorption edge determination: ZnO thin films as a model system (*Phys. Status Solidi B* 8/2015). *Physica Status Solidi B-basic Solid State Physics*, 252. <https://doi.org/10.1002/pssb.201552007>
- [39] Jothibas, M., Paulson, E., Mathivanan, A. et al. Biomolecules influences on the physiochemical characteristics of ZnO nanoparticles and its enhanced photocatalysis under solar irradiation. *Nanotechnol. Environ. Eng.* 8, 511–533 (2023). <https://doi.org/10.1007/s41204-023-00310-3>
- [40] Coulter, Jennifer B. & Birnie, Dunbar P. (2018). Assessing Tauc plot slope quantification: ZnO thin films as a model system. *Physica Status Solidi B* 255, 1700393. Retrieved from doi:10.7282/T3445QC7. <https://doi.org/10.1002/pssb.201700393>
- [41] Tripathy, N., Kim, DH. Metal oxide modified ZnO nanomaterials for biosensor applications. *Nano Convergence* 5, 27 (2018). <https://doi.org/10.1186/s40580-018-0159-9>
- [42] Droepenu Eric Kwabena, Boon Siong Wee, Chin Suk Fun, Kuan Ying Kok, Zaini Bin Assim, and Asare Ebenezer Aquisman, Comparative Evaluation of Antibacterial Efficacy of Biological Synthesis of ZnO Nanoparticles Using Fresh Leaf Extract and Fresh Stem-Bark of *Carica papaya*. *Nano Biomed. Eng.*, 2019, 11(3): 264-271. <https://doi.org/10.5101/nbe.v11i3.p264-271>
- [43] Farkas, N., Kramar, J.A. Dynamic light scattering distributions by any means. *J Nanopart Res* 23, 120 (2021). <https://doi.org/10.1007/s11051-021-05220-6>
- [44] R.Sagayaraj, T.Dhineshkumar, A.Prakash, S.Aravazhi, G.Chandrasekaran, D.Jayarajan, & S.Sebastian, Fabrication, Microstructure, Morphological and Magnetic Properties of W-type ferrite by Co-precipitation method: Antibacterial activity. *Chem. Phys. Lett* 759 (2020) 137944, <https://doi.org/10.1016/j.cplett.2020.137944>
- [45] Udhayan S, Udayakumar R, Sagayaraj R & Gurusamy K et al. Evaluation of Bioactive Potential of a *Tragia involucrata* Healthy Leaf Extract @ ZnO Nanoparticles. *BioNanoSci.* 11(2021)703-719. <https://doi.org/10.1007/s12668-021-00864-z>
- [46] R.Sagayaraj, S.Aravazhi, G.Chandrasekaran, Review on structural and magnetic properties of (Co–Zn) ferrite nanoparticles, *Int Nano Lett* 11(4) (2021) 307-319. <https://doi.org/10.1007/s40089-021-00343-z>
- [47] A.Prakash, R. Sagayaraj, D. Jayarajan, S. Aravazhi, G. Chandrasekaran, R. Nithya, Influence of Ce³⁺ Substitution on Magnetic Properties and Antibacterial Activity of Manganese Ferrite



Nanoparticles Synthesized by Coprecipitation Method, Asian Journal of Chemistry, 34 (2022) 2288-2296, <https://doi.org/10.14233/ajchem.2022.23840>

[48] Prakash, A., Sagayaraj, R., Jayarajan, D. *et al.* Influence of Ce^{3+} (Rare Earth Element) on the Structural, Morphological, Impedance, Binding Energy and Ferrimagnetic Properties of Spinel $ZnFe_2O_4$ Nanoparticles Fabricated by the Coprecipitation Method: Antibacterial Activity. Chemistry Africa (2022). <https://doi.org/10.1007/s42250-022-00570-7>

[49] D. Jayarajan, R. Sagayaraj, S.Silvan, S.Sebastian, R. Nithya, S. Sujeetha, Green synthesis, Structural and Magnetic Properties of $Mg_{0.5}Zn_{0.5}Fe_2O_4$ Ferrite Nanoparticles by the Coprecipitation Method: Averrhoa bilimbi fruit, Chemistry Africa, <https://doi.org/10.1007/s42250-023-00615-5>

[50] Munir, S., Liu, Z. W., Tariq, T., Rabail, R., Kowalczewski, P. Ł., Lewandowicz, J., ... & Aadil, R. M. (2022). Delving into the therapeutic potential of Carica papaya leaf against thrombocytopenia. Molecules, 27(9), 2760. <https://doi.org/10.3390/molecules27092760>

[51] Hampilos, K. E., Corn, J., Hodsdon, W., Anderes, E. N., Roop, R. P., Wagner, P., & Troy, L. R. (2015). Effect of Carica papaya leaf extract on platelet count in chronic immune thrombocytopenic purpura: a case series. <https://pubmed.ncbi.nlm.nih.gov/32549843/>

[52] Amitha Kurian, Preetham Elumalai (2021). Study on the impacts of chemical and green synthesized (Leucas aspera and oxy-cyclodextrin complex) dietary zinc oxide nanoparticles in Nile tilapia (Oreochromis nilotiucs). Environmental science and Pollution Research, <https://doi.org/10.1007/s11356-020-11992-6>